Life Sciences 232 (2019) 116613

Contents lists available at ScienceDirect

Life Sciences

journal homepage: www.elsevier.com/locate/lifescie

Valproic acid attenuates sepsis-induced myocardial dysfunction in rats by accelerating autophagy through the PTEN/AKT/mTOR pathway

Xiaohui Shi, Yan Liu, Daquan Zhang, Dong Xiao*

Department II of Critical Care Medicine, People's Hospital of Xinjiang Uygur Autonomous Region, Urumqi, China.

ARTICLE INFO

Keywords:
Valproic acid
Myocardial dysfunction
Sepsis
Autophagy
PTEN

ABSTRACT

Aims: Sepsis is a leading cause of death and disability worldwide. Autophagy may play a protective role in sepsis-induced myocardial dysfunction (SIMD). The present study investigated whether valproic acid (VPA), a class I histone deacetylase (HDAC) inhibitor, can attenuate SIMD by accelerating autophagy.

Main methods: A sepsis model was established via the cecum ligation and puncture of male Sprague–Dawley rats. Cardiac injuries were measured using serum markers, echocardiographic cardiac parameters, and hematoxylin and eosin staining. Cardiac mitochondria injuries were detected with transmission electron microscopy, adenosine triphosphate (ATP) and cardiac mitochondrial DNA (mtDNA) contents. Cardiac oxidative levels were measured using redox markers in the cardiac homogenate. Real-time polymerase chain reaction (RT-PCR) and Western blot were performed to detect the expression levels of relative genes and proteins. HDAC binding to the phosphatase and tensin homolog deleted on chromosome ten (PTEN) promoters and histone acetylation levels of the PTEN promoters were analyzed via chromatin immunoprecipitation and quantitative RT-PCR.

Key findings: VPA can ameliorate SIMD by enhancing the autophagy level of the myocardium to reduce mitochondrial damage, oxidative stress, and myocardial inflammation in septic rats. Moreover, this study demonstrated that VPA induces autophagy by inhibiting HDAC1- and HDAC3-mediated PTEN expression in the myocardial tissues of septic rats.

Significance: This study found that VPA attenuates SIMD through myocardial autophagy acceleration by increasing PTEN expression and inhibiting the AKT/mTOR pathway. These findings preliminarily suggest that VPA may be a potential approach for the intervention and treatment of SIMD.

1. Introduction

Sepsis is a complex systemic disease that involves life-threatening organ dysfunction caused by the body's uncontrolled response to infection [1]. The high incidence of sepsis, high mortality due to sepsis, and high hospitalization costs for sepsis are increasingly eliciting attention [2–5]. Sepsis-induced myocardial dysfunction (SIMD) is an overall but reversible dysfunction of the heart caused by sepsis and is an important cause of sepsis death in intensive care units [6–9]. However, no targeted treatment is currently available for SIMD, and its exact mechanism remains unclear [6,10]. An in-depth study of the pathogenesis and treatment of SIMD has important research significance to reduce high mortality due to sepsis.

The pathogenesis of SIMD is complex; it involves inflammatory mediator dysfunction, mitochondrial dysfunction, oxidative stress, calcium regulation disorder, autonomic nervous system disorders, and endothelial dysfunction [11,12]. Autophagy is a vital catabolic process in cells [13]. It is responsible for the degradation of biological macromolecules, aging and damaged organelles, and the reuse of degradation products [13]. A previous study found that autophagy can protect cardiomyocytes by degrading misfolded proteins and damaged organelles in cardiomyocytes, maintaining intracellular homeostasis, and ensuring energy supply to cardiomyocytes [14–16]. Therefore, the development of drugs related to the important targets of autophagy and its related pathways has important research significance for the prevention and treatment of SIMD. Histone acetylation modification is an important mechanism of epigenetic regulation. Previous studies have shown that histone deacetylase (HDAC) inhibitor plays a protective role in sepsis, but the underlying mechanisms remain unclear [17–21]. Prior research has also found that valproic acid (VPA), a class I HDAC inhibitor, can induce autophagy [22]. Therefore, we speculate that VPA may attenuate SIMD via autophagy.

Hence, this study investigated whether the HDAC inhibitor VPA can attenuate SIMD. We found that VPA can ameliorate SIMD by enhancing

* Corresponding author at: People's Hospital of Xinjiang Uygur Autonomous Region, N0. 91 Tianchi Road, Urumqi 830001, China.
E-mail address: dongxiao201904@126.com (D. Xiao).

https://doi.org/10.1016/j.lfs.2019.116613
Received 17 April 2019; Received in revised form 27 June 2019; Accepted 27 June 2019
Available online 29 June 2019
0024-3205/

the autophagy level of the myocardium to reduce myocardial inflammation, mitochondrial damage, and oxidative stress in sepsis animal models.

2. Materials and methods

2.1. Sepsis animal model

Male Sprague–Dawley rats (180–200 g) were acquired from the Animal Center of Xinjiang Medical University (Urumqi, China). The animals were housed in an environment with a constant temperature of 24 °C and a 12 h light–dark cycle. During treatment, the rats were randomly assigned to five groups: the sham group, the cecum ligation and puncture (CLP) group, the CLP + VPA (50 mg/kg) group, the CLP + VPA (100 mg/kg) group, and the CLP + VPA (200 mg/kg) group. A sepsis model was established via CLP as previously described [23,24]. The cecum of the rats in the CLP group was tightly ligated with 3–0 silk suture 1.2 cm to its distal end and perforated twice with a 22-gauge needle. The rats in the sham group were operated similarly but without ligation and puncturing of the cecum. The rats in the CLP + VPA groups were injected with their designated VPA concentration intraperitoneally. Meanwhile, the rats in the sham and CLP groups received an equivalent volume of sterile saline intraperitoneally. Rats were injected intraperitoneally with VPA (50, 100 or 200 mg/kg) and vehicle 2 h before and daily after CLP in the animal survival rate experiment (10 rats per group), and rats were monitored for 10 days after CLP. Rats were injected intraperitoneally with VPA (50, 100 or 200 mg/kg) and vehicle 2 h before CLP in other experiments (10 rats per group). All animal experimental protocols were approved by the Animal Research Ethics Committee of Xinjiang People's Hospital, and all procedures involving animals were performed in adherence to the Care and Use of Laboratory Animals (Committee for the Update of the Guide for the Care and Use of Laboratory Animals, 2011).

2.2. Cardiac injury marker detection

After 12 h of CLP, the echocardiographic cardiac parameters were determined as described earlier [25]. Briefly, rats were anesthetized by 2% isoflurane mixed with 0.5 L/min 100% O2 and placed on a warming pad (37 °C). Echocardiographic measurements were taken using a Vevo 2100 high-resolution in vivo imaging system (Visual Sonics Inc., Toronto, Canada). The left ventricular inner dimension (LVID) and ejection fraction (EF) were measured and assessed. The rats in each group were killed at 12 h post-CLP. Then, 2 mL blood sample was collected from each rat and centrifuged at 3000 ×g/min for 30 min to obtain the serum. The creatine kinase-MB (CK-MB) and lactate dehydrogenase (LDH) levels of the serum were determined using an automated analyzer (Abbott Architect, Abbott Park, Illinois, USA) as previously described [26]. The cardiac troponin I (cTnI) and cardiac myosin light chain-1 (cMLC1) concentrations of the serum were determined via ELISA assay following the manufacturer's protocol (Life Diagnostics Inc., USA).

2.3. Measurements of cardiac oxidative marker

After the rats in each group were killed, their heart tissues of the left ventricle were collected. The levels of reactive oxygen species (ROS), malondialdehyde (MDA), glutathione (GSH), and superoxide dismutase (SOD) in the cardiac homogenate of rats were determined using relevant commercial kits (Jiancheng, Nanjing, China). Briefly, the level of ROS was detected with Dihydroethidium (DHE) and the fluorescence was determined using a microplate reader (BioTek Instruments, Winooski, VT, USA) at excitation and emission wavelengths of 540 and 590 nm. The levels of MDA of the heart tissue of the left ventricle were determined by incubating with 10% Thiobarbituric acid (TCA) and 0.67% Thiobarbituric acid (TBA) and measured using 532 nm microplate reader (BioTek Instruments, Winooski, VT, USA). Hypoxanthine and xanthine oxidase were used as the superoxide generator, and nitro blue tetrazolium (NBT) was used as the superoxide indicator to measure the SOD level of heart tissue, which was measured using a 96-well plate reader (BioTek Instruments, Winooski, VT, USA) at 450 nm and the SOD activity was defined as U/mg protein. A GSH assay kit was applied to evaluate GSH activity. The homogenized heart tissue of the left ventricle tissue was centrifuged (10,000 ×g 15 min, 4 °C), and 0.6 mmol/L 5,5′-dithiobis (2-nitrobenzoic acid) (DTNB), 0.2 mg/mL Nicotinamide Adenine Dinucleotide Phosphate (NADPH), and glutathione reductase (GR) were mixed together to initiate the reaction.

2.4. Cardiac histological analysis

The animals in each group were killed at 12 h post-CLP. The hearts were perfused with cold saline and then 10% paraformaldehyde was administered. After fixation for 48 h, heart tissues of the left ventricle were embedded into paraffin, cut into sections (5 μm), and stained with hematoxylin and eosin (HE).

2.5. Transmission electron microscopy (TEM)

After the rats in each group were killed at 12 h post-CLP, their fresh heart tissues of the left ventricle were obtained, washed in phosphate buffered saline, cut into 1 mm cubes, and sequentially fixed in 4% glutaraldehyde and 4% osmium tetroxide for 24 h. Then, the samples were dehydrated in acetone and embedded into paraffin resin. Ultrathin sections were acquired using a microtome (Leica, Germany) and following standard procedures. The sections were stained with 1% uranyl acetate and 0.2% lead citrate and then analyzed using a transmission electron microscope (Hitachi, Japan). Images were acquired at 15000 × magnification.

2.6. Analysis of cardiac mitochondrial injury

The adenosine triphosphate (ATP) content of the rat's cardiac specimens was assessed using an enhanced ATP assay kit (Beyotime, Wuhan, China) following the manufacturer's instructions. The relative content of cardiac mitochondrial DNA (mtDNA) was measured via quantitative real-time polymerase chain reaction (qRT-PCR) using SYBR Green chemistry on a Quant Studio 7 Flex Real-Time PCR System (Applied Biosystems, Foster City, CA, USA). After the animals in each group were killed at 12 h post-CLP, the heart tissues of the left ventricle were collected and total DNA was extracted using the phenol-chloroform method. After the extracted DNA was diluted 10 times, it was used as a quantitative polymerase chain reaction (qPCR) template. Each sample was analyzed in triplicate at a final volume of 20 μL with iTaq SYBR Green Super mix PCR 1 × Master Mix (Bio-Rad Laboratories Inc., Hercules, CA, USA), 0.5 μM forward and reverse primers, and a DNA template. After 5 min of denaturation at 95 °C, amplification proceeded as follows: 40 cycles, with each cycle consisting of denaturation at 95 °C for 15 s, and annealing and extension at 60 °C for 34 s (fast block). The quantification of mtDNA content (mtDNA primer set) relative to nuclear DNA (β-actin primer set) was determined as previously reported [27]. The specific oligonucleotide primers used in this study were as follows: 5′-GGT TCT TAC TTC AGG GCC ATC A-3′ and 5′-TGA TTA GAC CCG TTA CCA TCG A-3′ for mtDNA, 5′-CCC AGC CAT GTA CGT AGC CA-3′ and 5′-CGT CTC CGG AGT CCA TCA C-3′ for β-actin.

2.7. Real-time polymerase chain reaction (RT-PCR)

The animals in each group were killed at 12 h post-CLP. The heart tissues of the left ventricle were collected. Total RNA was isolated via the trizol method and reverse transcribed using a one-step RT-PCR kit (Qiagen). The mRNA levels of the tumor necrosis factor-α (TNF-α),

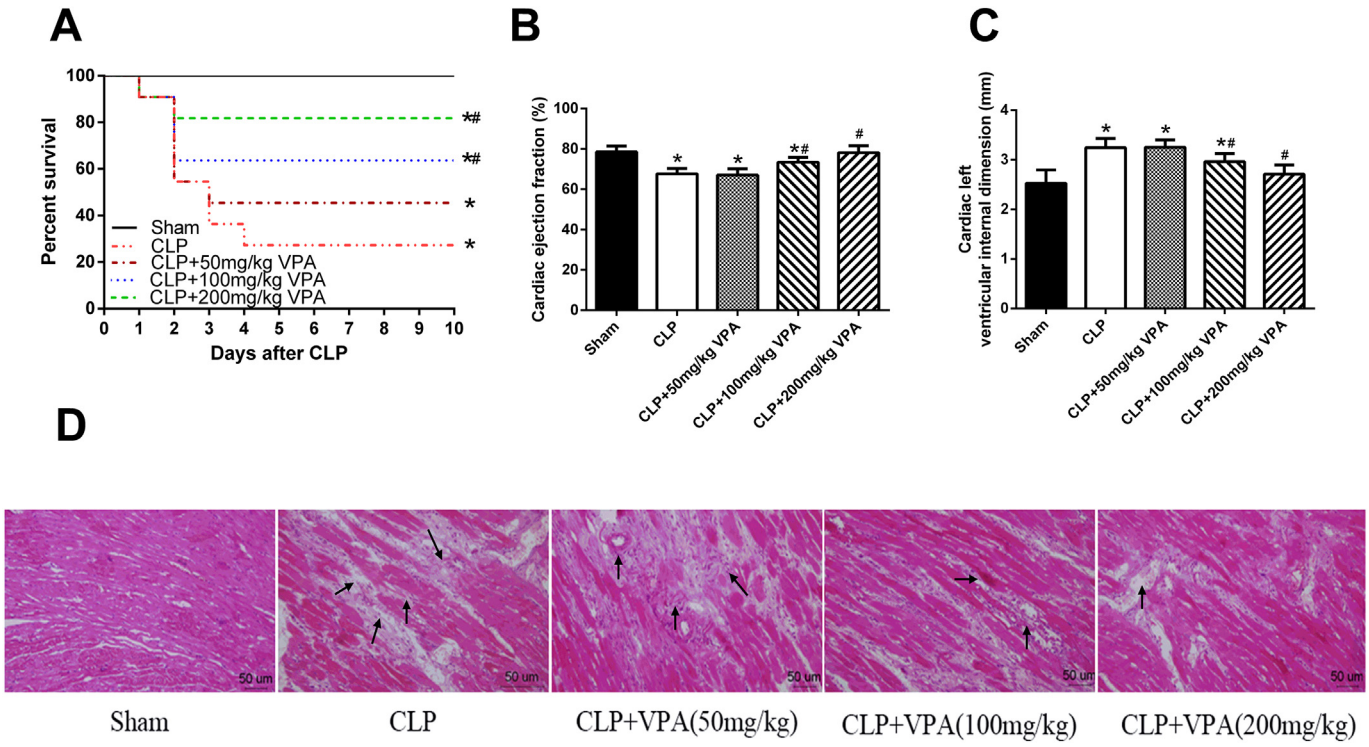

Fig. 1. VPA improves survival following CLP and CLP-induced cardiac dysfunction in rats. (A) Effect of VPA on survival following CLP in rats. Rats were injected intraperitoneally with VPA (50, 100 or 200 mg/kg) and vehicle 2 h before and daily after CLP. Animals were monitored for 10 days after CLP. (B) Effect of VPA on cardiac dysfunction following CLP in rats. Cardiac function parameters ejection fraction (EF) and left ventricular internal dimension (LVID) were measured by echocardiography. (C) Histological changes in the myocardial tissues at 12 h post-CLP (hematoxylin-eosin, ×40). The pathologic changes were shown with arrows. $^{*}P < 0.05$, significantly different from Sham, $\#P < 0.05$, significantly different from CLP (n = 10 per group).

interleukin 1β (IL-1β), matrix metalloproteinase-1 (MMP-1), matrix metalloproteinase-2 (MMP-2), and β-actin were detected via RT-PCR using SYBR Green chemistry on a Quant Studio 7 Flex RT-PCR System (Applied Biosystems, Foster City, CA, USA). Glyceraldehyde-3-phosphate dehydrogenase (GAPDH) was amplified under the same conditions to be used as internal control, which is unaffected by the treatment. The specific oligonucleotide primers used in this study were as follows: 5′-ATC CGA GAT GTG GAA CTG GC-3′ and 5′-CGA TCA CCC CGA AGT TCA GTA-3′ for TNF-α; 5′-CAA CAA AAA TGC CTC GTG C-3′ and 5′-TGC TGA TGT ACC AGT TGG G-3′ for IL-1β; 5′-AAA CCC TGA GTG CTA TG-3′ and 5′-TTT GGC AAA TAT GGT GTG-3′ for MMP-1; 5′-ACC GTC GCC CAT CAT CAA-3′ and 5′-CCT TCA GCA CAA AGA GGT TGC-3′ for MMP-2; and 5′-CAA GTT CAA CGG CAC AGT C-3′ and 5′-CAT ACT CAG CAC CAG CAT C-3′ for GAPDH.

2.8. Western blot

After the animals were killed, their heart tissues of the left ventricle were collected and homogenized in radio-immunoprecipitation assay lysis buffer (RIPA) (Biyuntian Biotechnology, Wuhan, China), and protein concentration was determined using a bicinchoninic acid protein assay kit (Beyotime, Wuhan, China) following the manufacturer's protocol. Extracted proteins (40 μg) were then separated via sodium dodecyl sulfate-polyacrylamide gel electrophoresis and transferred to polyvinylidene difluoride (PVDF) membranes (Merck, Millipore, Billerica, MA, USA). After blocking with 5% skimmed milk, the PVDF membranes were incubated with primary antibodies at 4 °C overnight. After three repeated washing with Tris-buffered saline-Tween (TBST), the membranes were probed with the corresponding horseradish peroxidase-conjugated secondary antibody for 1 h at room temperature. After three repeated washing with TBST, the membranes were detected via chemiluminescence and exposed on an X-ray film for autoradiography. The antibodies of TNF-α, IL-1β, MIP-1, MMP-2, H3 acetylated on Lys9 (Ac-H3K9), H4 acetylated at Lys12 (Ac-H4K12), Histone3, Histone4, HDAC1, HDAC2, HDAC3, HDAC8, LC3, p62, phosphatase and tensin homolog deleted on chromosome ten (PTEN), p-AKT, AKT, p-mTOR, mTOR, and β-actin were all purchased from Cell Signaling Technology (MA, USA).

2.9. Chromatin immunoprecipitation (ChIP) and qRT-PCR

After the animals were killed, the heart tissues of the left ventricle were collected, homogenized, and sonicated following the instructions in the ChIP assay kit (Abcam, Cambridge, MA, USA) used in the study. Then, the aliquots of the sheared chromatin solution were immunoprecipitated overnight at 4 °C with antibodies against Ac-H3K9, Ac-H4K12, HDAC1, and HDAC3. After incubation overnight, protein A agarose beads were added to each reaction to precipitate antibody complexes. Through qRT-PCR, PTEN promoter primers specific to PTEN promoters I-IV were used to validate the pulldown DNA fragments. Pulldown DNA from ChIP was measured via ultraviolet spectrophotometry. Approximately 60 ng DNA was utilized to perform qPCR with real-time PCR using SYBR Green chemistry on a Quant Studio 7 Flex Real-Time PCR System (Applied Biosystems, Foster City, CA, USA). Fold enrichment was calculated after normalization with input (no antibody added). The specific primers used for qPCR to sequences at the PTEN promoters were as follows: 5′-CAG GTC AGA AAT ACT TTA-3′ and 5′-TGT CGG TAA CTG ATC CAC-3′ for promoter I; 5′-CCT CAT TAA GCG GAG ATG-3′ and 5′-GCG AGC ACC CAC GAT AAC-3′ for promoter II; 5′-TGC GGC CTC ATG TAT TCC-3′ and 5′-AAC CGG TGG CGC TAG GTT-3′ for promoter III; and 5′-GGG TCA GAA CTT GGC CAC-3′ and 5′-AAG TAG AAA GCC CGT TTA-3′ for promoter IV.

2.10. Statistical analysis

Data were represented as mean ± standard deviation (SD) and

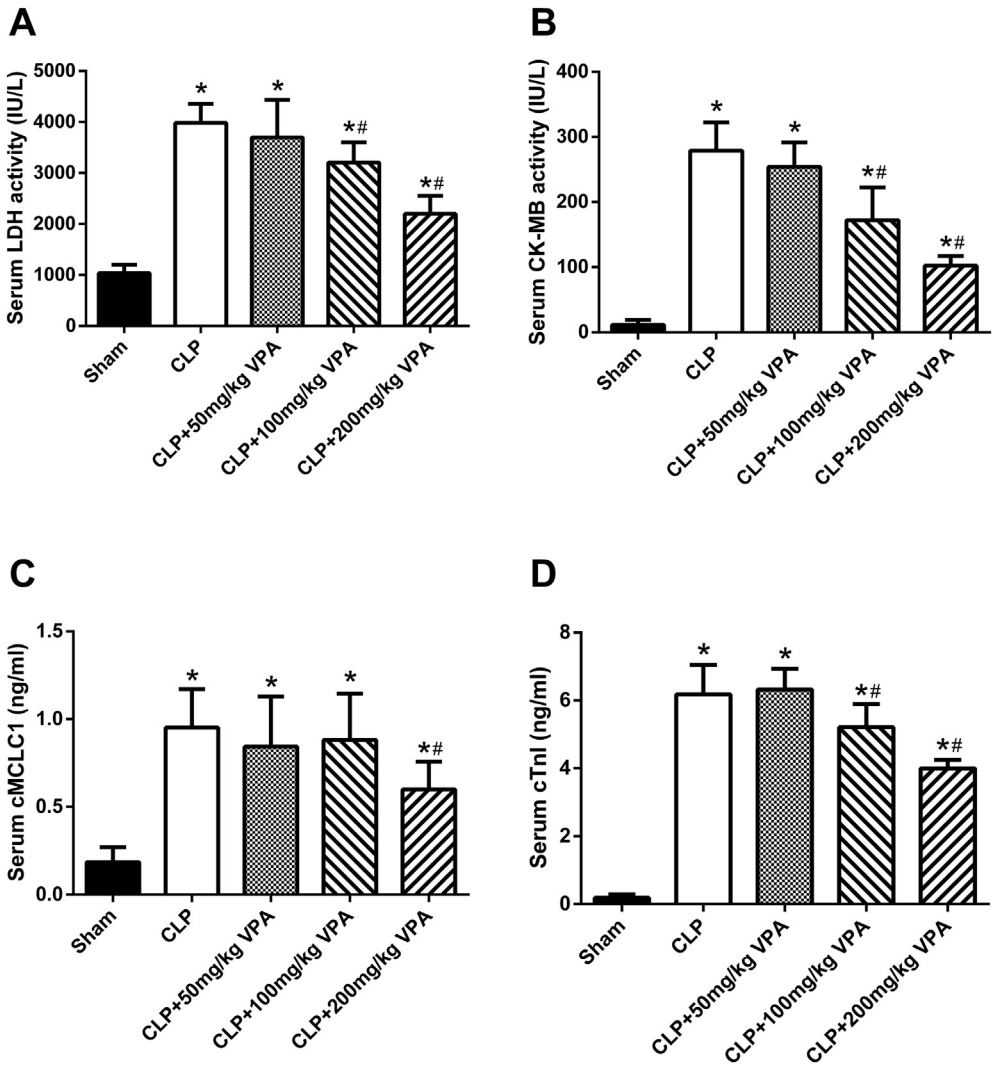

Fig. 2. VPA attenuates CLP-induced cardiac dysfunction. (A) Effect of VPA on serum LDH in rats. (B) Effect of VPA on serum CK-MB in rats. (C) Effect of VPA on serum cMLC1 in rats. (D) Effect of VPA on serum cTnI in rats. *$P < 0.05$, significantly different from Sham, #$P < 0.05$, significantly different from CLP (n = 10 per group).

were analyzed using GraphPad Prism software 6.02. Statistical analysis was performed using paired *t*-test or one-way ANOVA followed by Tukey's posttest. $P < 0.05$ was considered statistically significant.

3. Results

3.1. VPA attenuates mortality rate and myocardial damage in septic rats

SIMD is an overall but reversible dysfunction of the heart caused by sepsis; it is an important cause of sepsis death [11,12,28]. VPA was used to study the effects on sepsis-induced myocardial dysfunction in rats. The data showed that septic rats exhibited high mortality, and approximately 70% of the rats died within 4 days. However, 100 mg and 200 mg VPA treatment significantly reduced the 4-day mortality in septic rats (Fig. 1A). Cardiac function parameters, such as left ventricular structure and function, were also assessed via echocardiography [25]. CLP decreased EF and increased LVID, which was considerably attenuated by administering 100 mg and 200 mg VPA. This result indicated that VPA can improve myocardial function, which was decreased by CLP surgery (Fig. 1B and C). In addition, myocardial histopathological changes were observed to examine the protective effect of VPA on SIMD in rats at 12 h after CLP surgery. The morphology of cardiomyocytes was observed via HE staining. The sham operation group was found to have clear transverse stripes of myocardial fibers, but without degeneration, necrosis, and abnormal changes in the myocardial interstitial. Myocardial tissues obtained from the CLP group presented significant pathological changes, including evident degeneration of cardiomyocytes, swelling and partial fragmentation of the nucleus, partial rupture and dissolution of myocardial fiber, partial disappearance and interstitial edema of blurred myocardial stripes, and overflow of red blood cells. However, these pathological changes were significantly attenuated by 100 mg and 200 mg VPA treatment (Fig. 1D).

3.2. VPA attenuates myocardial injuries in septic rats

Serum LDH, CK-MB, cTnI, and cMLC1 are frequently used as biomarkers for acute heart disorders, particularly heart muscle cell death [26,29]. To detect the myocardial function of CLP-induced sepsis, serum LDH, CK-MB, cTnI, and cMLC1 levels were measured at 12 h after CLP surgery. The results showed that the serum LDH, CK-MB, cTnI, and cMLC1 levels significantly increased after CLP surgery. This result indicated that myocardial function was decreased in CLP-induced septic rats. However, VPA treatment significantly reduced all the aforementioned serum markers at a significant dose-dependent effect (Fig. 2A, B, C, and D). This finding indicated that VPA can decrease

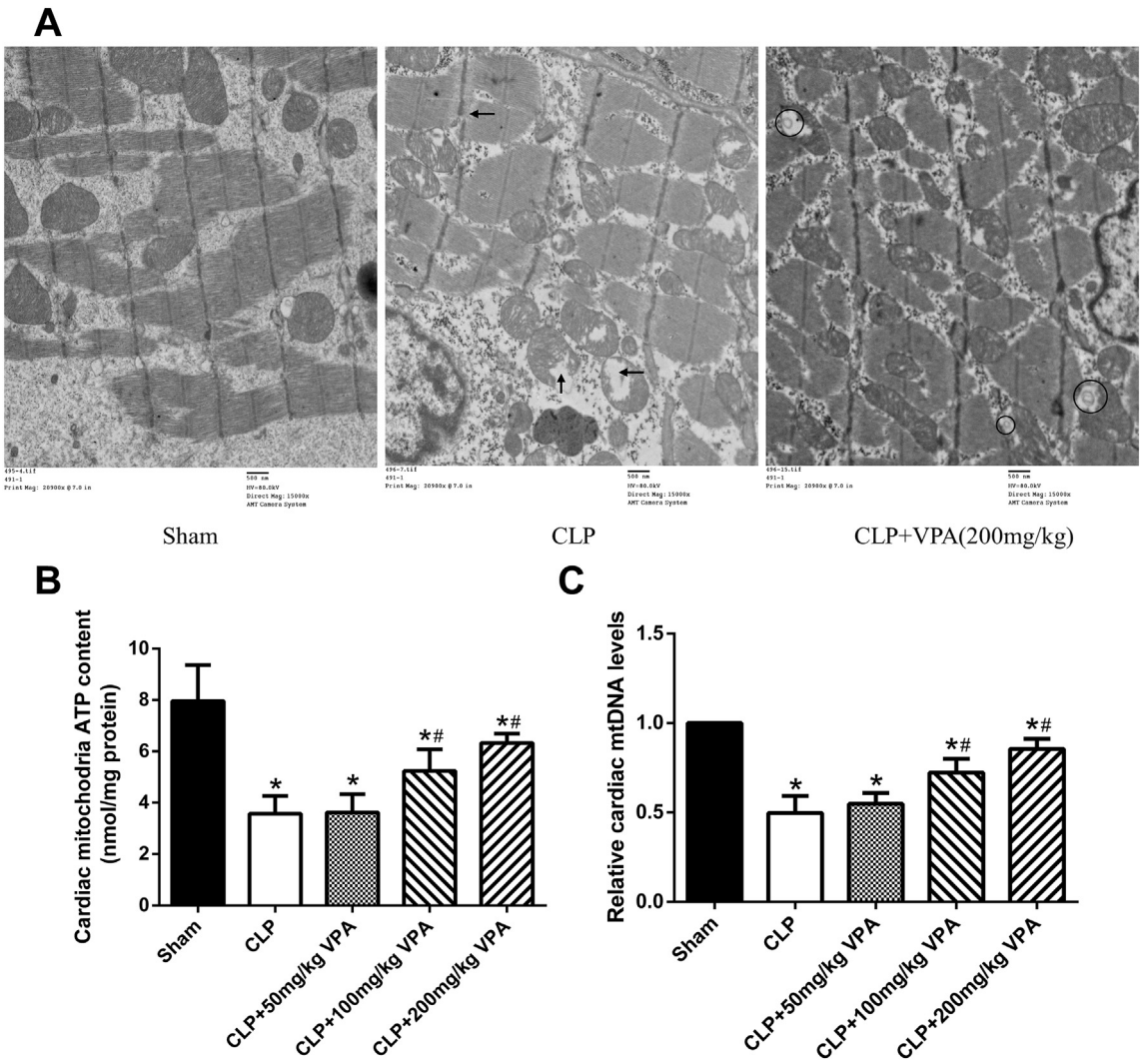

Fig. 3. VPA attenuates myocardial mitochondrial damage caused by CLP. (A) Transmission electron microscopy (TEM) images of myocardial tissues at 12 h post-CLP (×15,000). The myocardial mitochondrial damages such as swollen mitochondrion and fiber breakage were shown as arrows. The autophagosomes were circled. (B) ATP content in myocardial tissues at 12 h post-CLP. (C) Relative mtDNA content in myocardial tissues at 12 h post-CLP. $*P < 0.05$, significantly different from Sham, $\#P < 0.05$, significantly different from CLP (n = 10 per group).

myocardial injury and improve myocardial function.

3.3. VPA attenuates myocardial mitochondrial damage in septic rats

Myocardial histopathological changes were observed via TEM. In the CLP group, the number of myocardial mitochondria was significantly reduced. Abnormal mitochondrial size and arrangement, including visible swelling and vacuolar degeneration, were observed. A swollen mitochondrion can lead to the rupture of mitochondria. Myocardial cell boundaries were blurred, interstitial fiber structure increased significantly, and several areas of fiber breakage were dissolute. These pathological changes of the CLP group were also significantly attenuated by 200 mg VPA treatment (Fig. 3A). Moreover, we found that there were more autophagosomes in 200 mg VPA treatment group (circled in CLP + VPA group). Mitochondria are major sources of cellular ROS, which cause mitochondrial dysfunction and oxidative stress, and ultimately, cardiac damage [30]. ATP plays a crucial role in the normal physiological activities of cells and various pathophysiological processes. Abnormalities, such as cell degeneration, necrosis, and apoptosis, can decrease ATP levels; thus, the occurrence of mitochondrial dysfunction is suggested. Accordingly, the ATP levels of myocardial tissues were detected at 12 h after CLP surgery. The results showed that the ATP levels were significantly lower in the CLP group than in the sham operation control group. Meanwhile, 100 mg and 200 mg VPA treatment considerably increased the ATP levels at 12 h after CLP surgery (Fig. 3B). Considering that mtDNA content was reported to be affected by many factors to reflect mitochondrial dysfunction [27], we determined the relative mtDNA content in the heart via qPCR at 12 h after CLP surgery. A significant reduction was observed in the CLP group. Such reduction demonstrated the sepsis-related loss of mtDNA in rat heart. However, 100 mg and 200 mg VPA treatment substantially increased mtDNA loss at 12 h post-CLP surgery (Fig. 3C).

3.4. VPA decreases oxidative damage of myocardial mitochondrial damage in septic rats

Oxidative stress is a predominant component involved in the pathogenesis of SIMD [11]. Hence, the ROS of myocardial tissues were detected at 12 h after CLP surgery. The results showed that ROS levels were significantly higher in the CLP group than in the sham operation control group. Meanwhile, 100 mg and 200 mg VPA treatment considerably decreased ROS levels at 12 h after CLP surgery (Fig. 4A). MDA is one of the final products of ROS attack in phospholipids and is

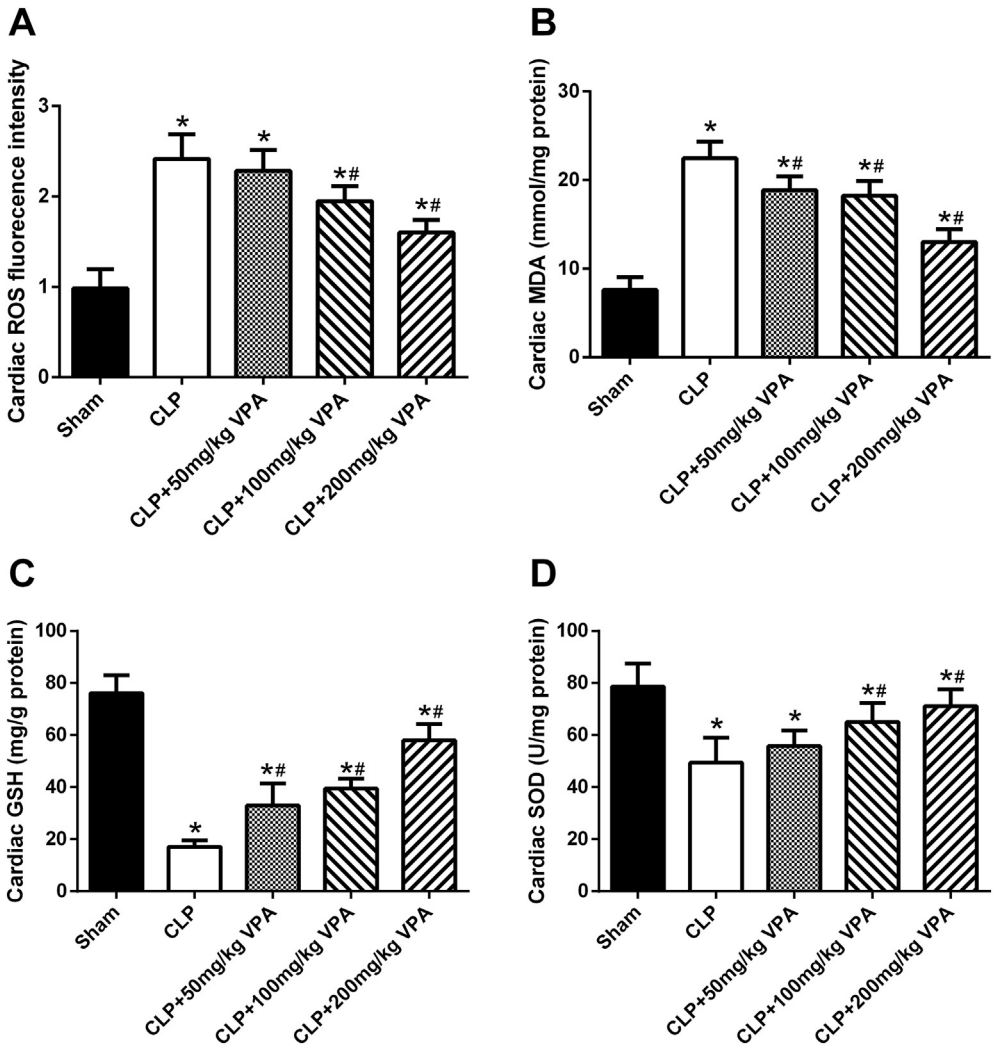

Fig. 4. VPA attenuates myocardial oxidative stress injury caused by CLP. (A) The level of ROS in myocardial tissues. (B) The level of MDA in myocardial tissues. (C) The level of GSH in myocardial tissues. (D) The level of SOD in myocardial tissues. *$P < 0.05$, significantly different from Sham, #$P < 0.05$, significantly different from CLP (n = 10 per group).

responsible for cell membrane damage [31]. Therefore, the MDA levels of the myocardial tissues were also detected at 12 h after CLP surgery. As shown in Fig. 3B, the MDA levels of the CLP group were significantly higher than those of the sham operation control group. However, 50, 100, and 200 mg VPA treatment could significantly decrease the MDA levels at 12 h after CLP surgery (Fig. 4B). The SOD activity and GSH exhibit antioxidative ability for cell damage. Thus, the SOD activity and GSH levels of myocardial tissues were measured at 12 h after CLP surgery (Fig. 4C and D). The results showed that GSH levels were significantly lower in the CLP group than in the sham operation control group. Meanwhile, 50, 100, and 200 mg VPA treatment considerably increased GSH levels at 12 h post-CLP surgery. SOD activity also decreased in the CLP group, and 100 mg and 200 mg VPA treatment substantially increased SOD activity at 12 h after CLP surgery. Overall, these results showed that VPA treatment remarkably decreased the oxidative damage of myocardial damage in septic rats.

3.5. VPA decreases the expression of inflammatory cytokines in septic rats

Inflammatory response plays an important role in the development of sepsis. ROS can directly or indirectly elevate inflammation and trigger the expression of inflammatory cytokines [32]; hence, the TNF-α, IL-1β, MMP-1, and MMP-2 levels in myocardial tissues were measured via qPCR and Western blot analysis at 12 h after CLP surgery. As shown in Fig. 5, the TNF-α, IL-1β, MMP-1, MMP-2 mRNA, and protein levels significantly increased at 12 h after CLP surgery. Meanwhile, 100 mg and 200 mg VPA treatment considerably decreased inflammatory cytokines at 12 h after CLP surgery.

3.6. VPA accelerates myocardial autophagy in septic rats

LC3 is an autophagic marker. When autophagy is initiated, cytosolic LC3 (i.e., LC3-I) will enzymatically cleave a small segment of the polypeptide and transform it into an autophagosome membrane type (i.e., LC3-II); hence, the LC3-II/LC3-I ratio can be used to estimate autophagy level. P62 is another autophagy marker protein. When autophagy occurs, a reduction in p62 protein level indicates an increase in autophagic flux, whereas an increase in p62 protein level indicates that the autophagy/lysosomal degradation pathway is inhibited and autophagic flux is reduced [13]. Therefore, the LC3-II/LC3-I ratio and p62 levels in myocardial tissues were measured via Western blot analysis at 12 h after CLP surgery. The results showed that the LC3-II/LC3-I ratio increased at 12 h after CLP surgery. Meanwhile, 100 mg and 200 mg VPA treatment significantly increased the LC3-II/LC3-I ratio at 12 h after CLP surgery. As shown in Figs. 6A and 6B, 100 mg and 200 mg VPA treatment considerably decreased the reduction in p62 protein levels at 12 h after CLP surgery. These results showed that VPA accelerated the autophagy of myocardial damage in septic rats.

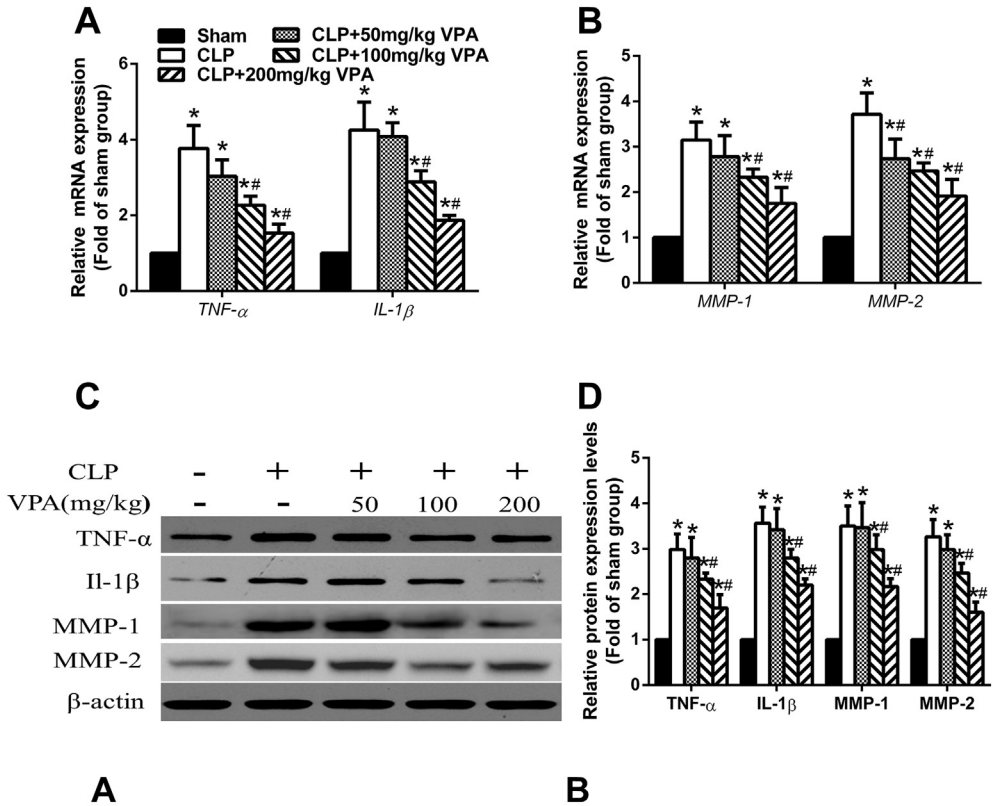

Fig. 5. VPA attenuates CLP-induced cardiac proinflammatory cytokines. (A, B) Cardiac inflammation markers TNF-α, IL-1β, MIP-1, and MIP-2 were measured by real-time PCR. $*P < 0.05$, significantly different from Sham, $\#P < 0.05$, significantly different from CLP (n = 3 per group). (C, D) Cardiac inflammation markers TNF-α, IL-1β, MIP-1, and MIP-2 were measured by western blotting. $*P < 0.05$, significantly different from Sham, $\#P < 0.05$, significantly different from CLP (n = 6 per group).

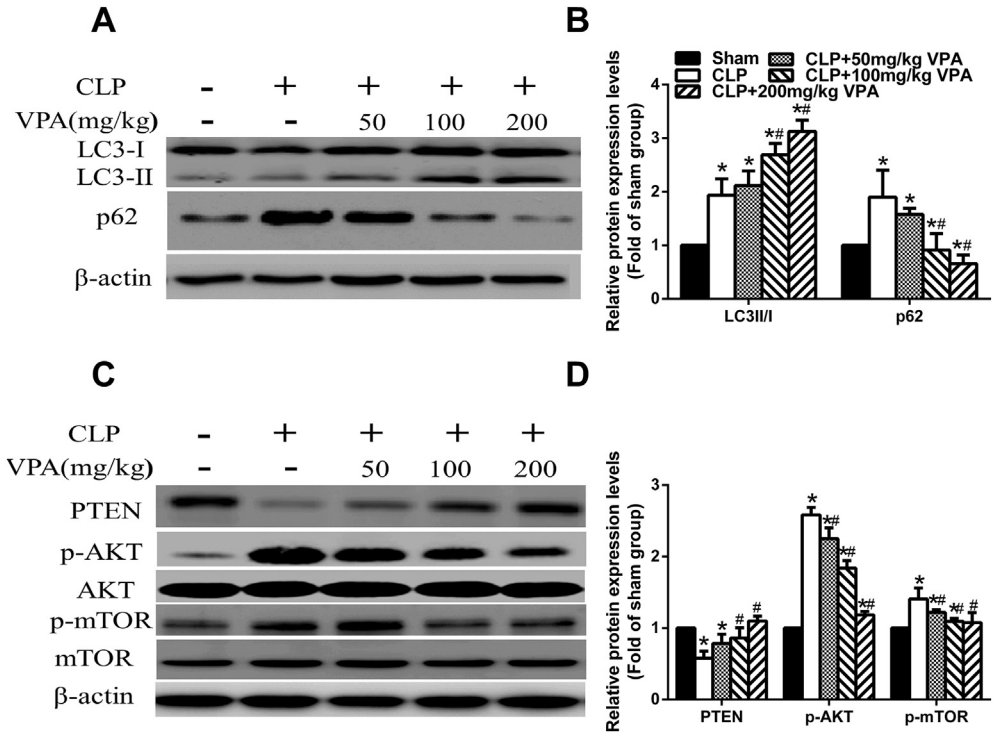

Fig. 6. VPA accelerates myocardial autophagy and autophagy-related signal pathway. (A, B) Effect of VPA on myocardial autophagy. Western blot analyses of two autophagy markers LG 3 and p62 along with control protein β-actin. (C, D) Effect of VPA on the autophagy-related signal pathway. $*P < 0.05$, significantly different from Sham, $\#P < 0.05$, significantly different from CLP (n = 6 per group).

The phosphatidylinositol 3-kinase (PI3K)/AKT/mTOR signaling pathway plays an important role in autophagy [33]. AKT can activate its downstream mTOR to inhibit the occurrence of autophagy. Thus, the phosphorylation of AKT and mTOR was investigated in this study. As shown in Fig. 6C and D, the phosphorylation levels of AKT and mTOR in the myocardial tissues were significantly increased. Meanwhile, 50, 100, and 200 mg VPA treatment considerably decreased the phosphorylation levels of AKT and mTOR at 12 h after CLP surgery. PTEN is a negative inhibitor of the PI3K/AKT/mTOR signaling pathway [34]; hence, the expression of PTEN was measured in this study. The data showed that the expression of PTEN in the myocardial tissues of septic rats was significantly decreased. Meanwhile, 100 mg and 200 mg VPA treatment substantially increased the phosphorylation levels of AKT and mTOR at 12 h after CLP surgery. Overall, these data showed that VPA may accelerate myocardial autophagy by increasing the expression of PTEN and inhibiting the PTEN downstream AKT/mTOR signaling pathway.

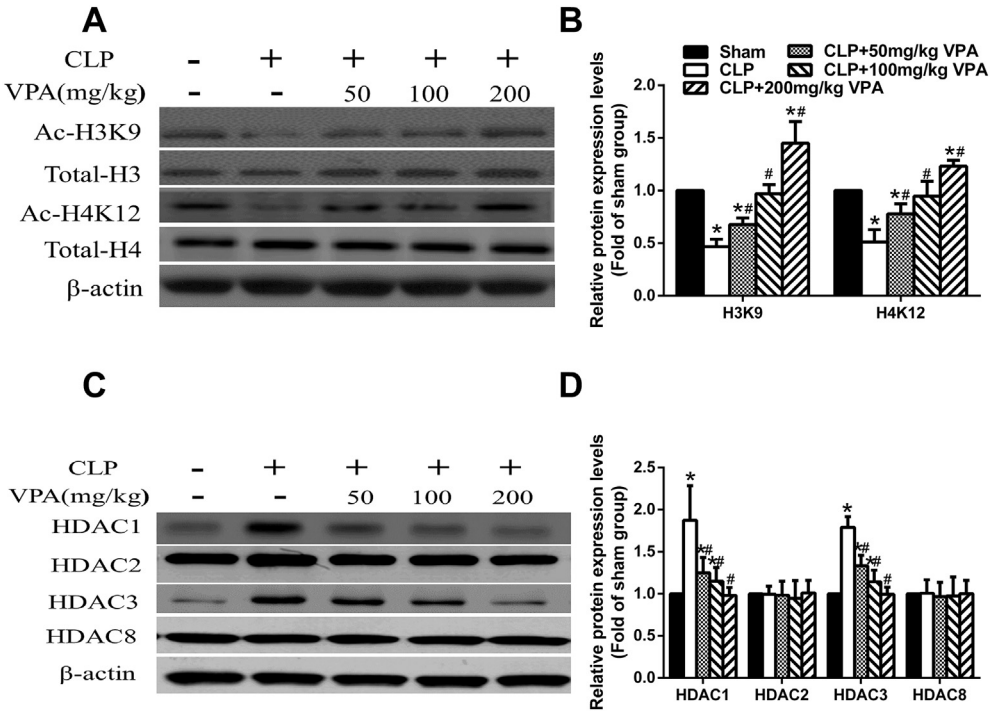

Fig. 7. VPA inhibits HDAC expression and increases histone acetylation levels in myocardial tissue. (A, B) VPA increases histone acetylation levels in myocardial tissue 12 h after CLP. Western blot analyses of Ac-H3K4, total-H3, Ac-H4K12 and total-H4 along with control protein β-actin. (C, D) VPA inhibits HDAC expression in myocardial tissues. Western blot analyses of HDAC1, HDAC2, HDAC3, and HDAC8 along with control protein β-actin. $*P < 0.05$, significantly different from Sham, $\#P < 0.05$, significantly different from CLP (n = 6 per group).

3.7. VPA improves the abnormality of histone acetylation and HDAC levels in septic rats

VPA is an approved anticonvulsant and mood-stabilizing drug with a long history of clinical use; it also belongs to class I HDAC inhibitors. Hence, the levels of histone acetylation and class I HDAC expression were measured in the myocardial tissues at 12 h after CLP surgery. As shown in Figs. 7A and 7B, 50, 100, and 200 mg VPA treatment significantly increased the reduction of Ac-H3K9 and Ac-H4K12 at 12 h after CLP surgery. HDAC1 and HDAC3 levels in the myocardial tissues were considerably increased. Meanwhile, 50, 100, and 200 mg VPA treatment remarkably decreased HDAC1 and HDAC3 levels at 12 h after CLP surgery (Fig. 7C and D). No significant difference in HDAC2 and HDAC8 levels were observed in myocardial tissues among the groups.

3.8. VPA increases myocardial PTEN expression through the histone acetylation mechanism in septic rats

To further clarify the mechanism of the PTEN expression of VPA, a class I HDAC inhibitor, i.e., ChIP, and qPCR were used to measure HDAC binding to the PTEN promoters and the histone acetylation levels of the PTEN promoters in myocardial tissues. The results showed that the binding of HDAC1 to PTEN promoters I–III increased dramatically in myocardial tissues at 12 h after CLP; however, VPA significantly decreased HDAC1 binding to PTEN promoters I–III at a dose-dependent treatment (Fig. 8B). In addition, the data also showed that VPA considerably decreased HDAC3 binding to PTEN promoters I, II, and IV at a dose-dependent treatment (Fig. 8C). Moreover, the ChIP and qPCR analysis with Ac-H3K9 and Ac-H4K12 antibodies showed that the histone acetylation levels of PTEN promoters I–IV decreased dramatically in myocardial tissues at 12 h after CLP. Meanwhile, VPA significantly increased histone acetylation levels of PTEN promoters I–IV at a dose-dependent treatment (Fig. 8D and E). All these data showed that VPA can regulate the expression of PTEN through the histone acetylation mechanism as a class I HDAC inhibitor.

4. Discussion

The current interventions that target autophagy in the treatment of SIMD remain lacking. The major findings of the current study showed that VPA, a first class HDAC inhibitor, can attenuate SIMD by promoting autophagy to improve mitochondrial function, reduce oxidative damage, and decrease excessive immune response. Moreover, the current study showed that VPA can inhibit the AKT signaling pathway, further inhibit p-mTOR, and consequently, increased autophagic levels and excessive immune response. These results preliminarily indicated that VPA may be used for the intervention and treatment of SIMD.

The CLP method is a classic animal model of sepsis [23,24]; hence, it was used in the present study to clarify the mechanism of SIMD. Firstly, we observed the effect of CLP on the survival rate of rats. We found that rats began to die after 12 h of CLP, so we chose the 12-hour time point to observe the improvement of myocardial damage by VPA treatment. The myocardial histopathological changes observed via HE staining and TEM; the cardiac injury markers of serum LDH, CK, cTnI, and cMLC1 levels; and the echocardiography of EF and LVID showed that CLP leads to SIMD. These results are consistent with those of a previous study [35]. As expected, VPA significantly attenuated the injury markers of SIMD in a dose-dependent manner; thus, VPA increased the survival rate of septic rats.

Mitochondrial dysfunction plays a significant role in the pathogenesis of sepsis, and its association with a decrease in myocardial ATP content is likely correlated with the deterioration of myocardial function during the late stage of sepsis [11,30]. Our results found that sepsis-induced mitochondrial swelling, iliac crest loss, and vacuolar degeneration. It further caused cardiomyocyte mitochondrial dysfunction by reducing ATP and mtDNA loss. Meanwhile, VPA significantly increased the reduction of ATP and the loss of mtDNA to attenuate cardiomyocyte mitochondrial dysfunction. Mitochondria are major sources of cellular ROS, which lead to mitochondrial dysfunction, oxidative stress, and ultimately, cardiac damage [11]. Our data showed that VPA can decrease the ROS levels and MDA of the final products of ROS at 12 h after CLP surgery. We also found that VPA can improve the redox protection system of the myocardium, such as SOD and GSH. Although early myocardial dysfunction during sepsis is associated with

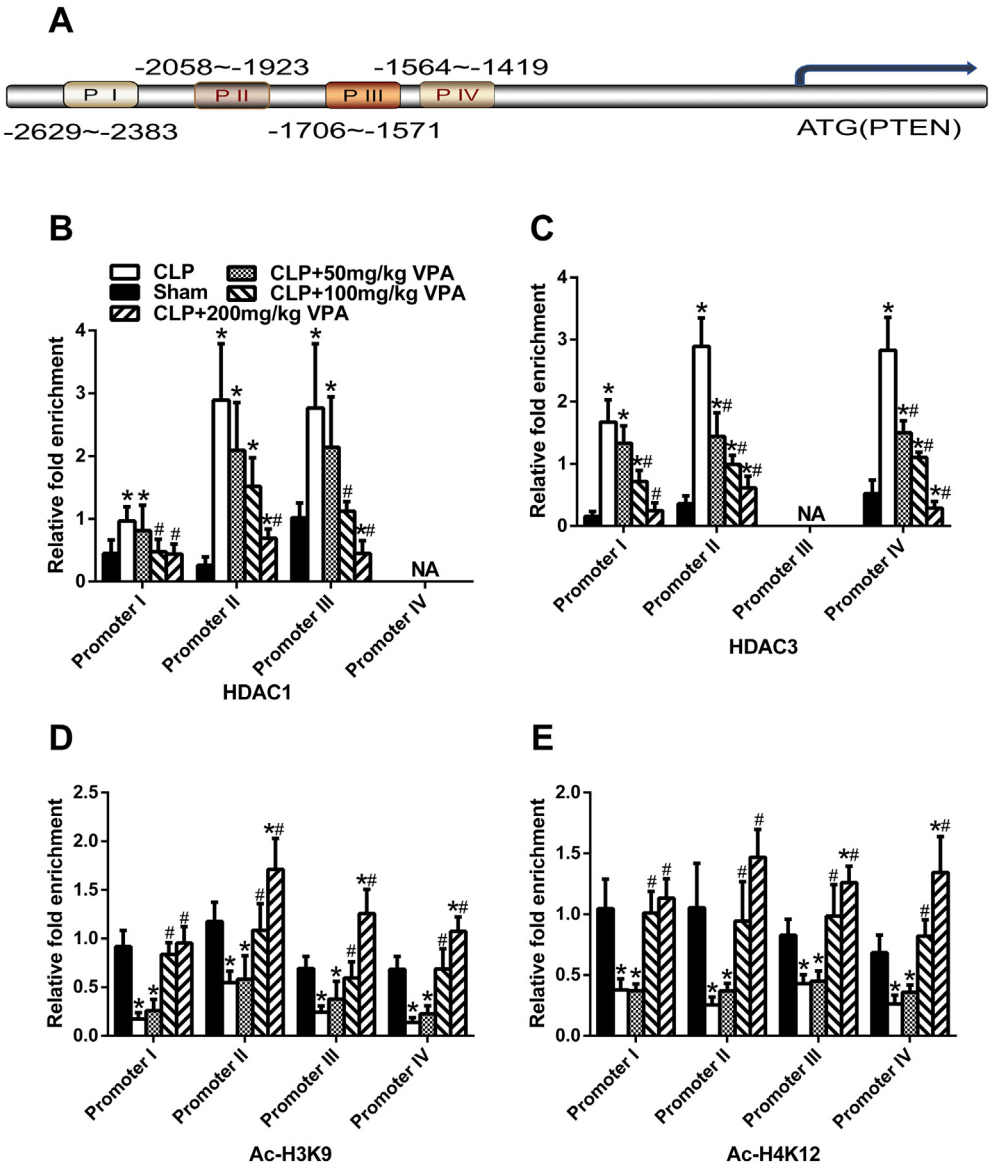

Fig. 8. VPA inhibits HDAC binding to the PTEN promoters and increases histone acetylation levels of the PTEN promoters in myocardial tissue. (A) Diagram of PTEN promoters. (B, C) VPA inhibits HDAC1 and HDAC3 binding to the PTEN promoters in myocardial tissues. HDAC binding to the PTEN promoters was measured by Chromatin immunoprecipitation (ChIP) and real-time PCR. (D, E) VPA increases histone acetylation levels of the PTEN promoters in myocardial tissues. The Ac-H3K9 and Ac-H4K12 levels of the PTEN promoters were measured by Chromatin immunoprecipitation (ChIP) and real-time PCR. $^{*}P < 0.05$, significantly different from Sham, $\#P < 0.05$, significantly different from CLP (n = 3 per group).

myocardial inflammation rather than mitochondrial injury, oxidative stress caused by subsequent mitochondrial damages exacerbated the immune response and caused myocardial damage. Interestingly, this study found that VPA treatment significantly decreased TNF-α, IL-1β, MMP-1, and MMP-2 at 12 h after CLP surgery. Consistent with previous studies [30,36,37], the results showed that mitochondrial damage is the main pathological factor of SIMD. Meanwhile, VPA can improve mitochondrial function, reduce oxidative damage, and decrease the excessive immune response to attenuate SIMD.

Autophagy is the process of delivering damaged proteins and organelles to maintain cellular homeostasis or be involved in cell death [13]. Autophagy is activated in the heart during sepsis; however, whether it is protective or detrimental remains unclear. Several previous studies have shown that promoting autophagy can protect cardiomyocytes from lipopolysaccharide-induced cell death, whereas inhibiting autophagy achieved the opposite result [38–40]. We speculate that autophagy can eliminate mitochondrial damage, and thus, reduce oxidative stress and excessive immune response. As expected, VPA can significantly change the LC3-II/LC3-I ratio and the reduction of the p62 protein levels at 12 h after CLP surgery. The results showed that VPA can accelerate autophagy to reduce myocardial damage in septic rats.

The role of the PI3K/Akt signaling pathway in myocardial disorders of sepsis is complicated. Several studies have shown that inhibiting the PI3K/Akt pathway can attenuate myocardial injury [41–44]. By contrast, other studies have found that promoting the PI3K/Akt pathway can reduce myocardial damage [45,46]. This finding may suggest that the PI3K/Akt signaling pathway plays different roles at various stages of SIMD, similar to autophagy having two sides in cell death. Here, we found that Akt was activated at 12 h after CLP and VPA treatment inhibited the AKT signaling pathway; this result is consistent with those of previous studies [43–45]. mTOR is the downstream substrates of AKT, and mTOR activation by AKT will inhibit autophagy. Further study found that VPA can inhibit mTOR activation to accelerate autophagy. We also determined that VPA, a first class of HDAC inhibitor, significantly decreased HDAC1 and HDAC3 levels at 12 h after CLP surgery. The lipid phosphatase, PTEN, acted as an endogenous negative regulator of the PI3K/Akt pathway [34]. Therefore, the effect of VPA on the expression of PTEN was studied. Interestingly, we found that VPA can regulate the expression of PTEN as a class I HDAC inhibitor. These data are consistent with previous studies, and VPA can upregulate PTEN transcription and expression, and augment the dephosphorylation of PIP3 [47–49]. Moreover, this study found that VPA inhibits HDAC1 and HDAC3 binding to PTEN promoters, increases the histone acetylation levels of PTEN promoters, and consequently,

increases the expression of PTEN in myocardial tissues. However, we only found that HDAC1 and HDAC3 significantly reduced in CLP model rats. The exact mechanism of CLP leading to the decrease of HDAC1 and HDAC3 deserves further study. In addition, VPA was studied as a first class HDAC inhibitor in SIMD in this research. Several previous studies have shown that other HDAC inhibitors may also play important roles in sepsis; hence, the roles of other HDACs and inhibitors in SIMD are also worthy of further study [50–53]. After all, this study found that VPA could improve SIMD through epigenetic mechanisms. This research will provide a new perspective on the development of SIMD interventions.

5. Conclusion

The salient finding of the present study is that VPA attenuates SIMD by promoting autophagy to improve mitochondrial function, reduce oxidative damage, and decrease excessive immune response. Moreover, this study demonstrated that VPA induces autophagy by inhibiting HDAC1- and HDAC3-mediated PTEN expression in the myocardial tissues of septic rats. These results preliminarily indicated that VPA may be used for the intervention and treatment of SIMD.

Author contributions

Conception and design: Xiaohui Shi and Dong Xiao. Acquisition of data: Xiaohui Shi and Yan Liu. Analysis and interpretation of data: Xiaohui Shi and Daquan Zhang. Writing, review, and revision of the manuscript: Xiaohui Shi, Daquan Zhang, and Dong Xiao.

Funding

This research did not receive any specific grant from funding agencies in the public, commercial, or not-for-profit sectors.

Declaration of Competing Interest

The authors declare that they have no competing interests.

References

[1] S. M, D. CS, S. CW, S.-H. M, A. D, B. M, B. R, B. GR, C. JD, C. CM, H. RS, L. MM, M. JC, M. GS, O. SM, R. GD, v.d.P. T, V. JL, A.D.J, The third international consensus definitions for sepsis and septic shock (Sepsis-3), JAMA. 315(8) (2016) 801–810. doi:https://doi.org/10.1001/jama.2016.0287.
[2] S.D.L.R. A, G. F, M.E.J.A.o.t, Epidemiologic trends of sepsis in western countries, Medicine 4 (17) (2016) 325, https://doi.org/10.21037/atm.2016.08.59.
[3] G. E, M. DR, K. Z, S. CA, V. C, L.M.J.I.j.o.a, Antimicrobial resistance prevalence, rates of hospitalization with septicemia and rates of mortality with sepsis in adults in different US states, Agents. 6 (2019) pii: S0924-8579(19)30056-1. doi:https://doi.org/10.1016/j.ijantimicag.
[4] K. J, K. K, L. H, A.S.J. Clinical, e.e, Epidemiology of sepsis in Korea: a population-based study of incidence, mortality, cost and risk factors for death in sepsis, Medicine. 6(1) (2019) 49–63. doi:10.15441/ceem.18.007.
[5] Y. Y., J.F. X., K.J. Y., C. Y., J.G. L., X.D. G., J. Y., X.C. M., Y. K., C.S. Y., X.Q. Y., H.C. S., H.B. Q., Epidemiological study of sepsis in China: protocol of a cross-sectional survey, Chin. Med. J. 129 (24) (2016) 2967–2973, https://doi.org/10.4103/0366-6999.195474.
[6] A. E, F. E, D. K, T. FS, F. F, S.S, Myocardial depression in sepsis: from pathogenesis to clinical manifestations and treatment, J. Crit. Care. 29(4) (2014) 500–511. doi:https://doi.org/10.1016/j.jcrc.
[7] W. J, H. S, S. M, B. S, G. F, M. S, M. S, Z. J, B. S, A. M, K. T, F. R, L. H, M.-W. U, E. H, W. K, Severity of cardiac impairment in the early stage of community-acquired sepsis determines worse prognosis, Clin. Res. Cardiol. 102(10) (2013) 735–744. doi:https://doi.org/10.1007/s00392-013-0584-z.
[8] E. RR, S. AN, F. MJ, S. RL, R. CA, A. A, L. P, Pathophysiology, echocardiographic evaluation, biomarker findings, and prognostic implications of septic cardiomyopathy: a review of the literature, Crit. Care 22 (1) (2018) 112, https://doi.org/10.1186/s13054-018-2043-8.
[9] O. SR, P. JN, M. M, G. S, S. JN, K. GC, O.J, Outcome prediction in sepsis: speckle tracking echocardiography based assessment of myocardial function, Crit. Care. 18(4) (2014) R149. doi:https://doi.org/10.1186/cc13987.
[10] K. Y, I. T, N. M, Y. K, Y.T, Sepsis-induced myocardial dysfunction: pathophysiology and management, J. Intensive Care. 4 (2016) 22. doi:https://doi.org/10.1186/s40560-016-0148-1.
[11] X. Lv, H. Wang, Pathophysiology of sepsis-induced myocardial dysfunction, Mil Med Res 3 (2016) 30, , https://doi.org/10.1186/s40779-016-0099-9.
[12] R.W. Morgan, J.C. Fitzgerald, S.L. Weiss, V.M. Nadkarni, R.M. Sutton, R.A. Berg, Sepsis-associated in-hospital cardiac arrest: epidemiology, pathophysiology, and potential therapies, J. Crit. Care 40 (2017) 128–135, https://doi.org/10.1016/j.jcrc.2017.03.023.
[13] D. J, B. E, Life, death and autophagy, Nat. Cell Biol. 20 (10) (2018) 1110–1117, https://doi.org/10.1038/s41556-018-0201-5.
[14] Z. E, Z. X, Z. L, L. N, Y. J, T. K, Y. R, H. J, Z. M, S. D, H. L, Minocycline promotes cardiomyocyte mitochondrial autophagy and cardiomyocyte autophagy to prevent sepsis-induced cardiac dysfunction by Akt/mTOR signaling, Apoptosis (2019), https://doi.org/10.1007/s10495-019-01521-3.
[15] B.-S.P. JM, K. G, G.L, Autophagy and mitophagy in cardiovascular disease, Circ. Res.. 120(11) (2017) 1812–1824. doi:https://doi.org/10.1161/CIRCRESAHA.117.311082.
[16] S. Lavandero, M. Chiong, B.A. Rothermel, J.A. Hill, Autophagy in cardiovascular biology, J. Clin. Invest. 125 (1) (2015) 55–64, https://doi.org/10.1172/JCI73943.
[17] E. Ciarlo, A. Savva, T. Roger, Epigenetics in sepsis: targeting histone deacetylases, Int. J. Antimicrob. Agents 42 (Suppl) (2013) S8–12, https://doi.org/10.1016/j.ijantimicag.2013.04.004.
[18] M.H. Ji, G.M. Li, M. Jia, S.H. Zhu, D.P. Gao, Y.X. Fan, J. Wu, J.J. Yang, Valproic acid attenuates lipopolysaccharide-induced acute lung injury in mice, Inflammation 36 (6) (2013) 1453–1459, https://doi.org/10.1007/s10753-013-9686-z.
[19] S.J. Kim, J.S. Park, D.W. Lee, S.M. Lee, Trichostatin A protects liver against septic injury through inhibiting toll-like receptor signaling, Biomol Ther (Seoul) 24 (4) (2016) 387–394, https://doi.org/10.4062/biomolther.2015.176.
[20] J. Thangavel, S. Samanta, S. Rajasingh, B. Barani, Y.T. Xuan, B. Dawn, J. Rajasingh, Epigenetic modifiers reduce inflammation and modulate macrophage phenotype during endotoxemia-induced acute lung injury, J. Cell Sci. 128 (16) (2015) 3094–3105, https://doi.org/10.1242/jcs.170258.
[21] L. Zhang, S. Jin, C. Wang, R. Jiang, J. Wan, Histone deacetylase inhibitors attenuate acute lung injury during cecal ligation and puncture-induced polymicrobial sepsis, World J. Surg. 34 (7) (2010) 1676–1683, https://doi.org/10.1007/s00268-010-0493-5.
[22] J. MM, W. L, Z. Q, X. W, Z. Y, Z. X, X. PP, S. Y, L. H, J. A, C. S, Z.W.J., Induction of autophagy by valproic acid enhanced lymphoma cell chemosensitivity through HDAC-independent and IP3-mediated PRKAA activation, Autophagy. 11(12) (2015) 2160–2171. doi:https://doi.org/10.1080/15548627.2015.1082024.
[23] L. Dejager, I. Pinheiro, E. Dejonckheere, C. Libert, Cecal ligation and puncture: the gold standard model for polymicrobial sepsis? Trends Microbiol. 19 (4) (2011) 198–208, https://doi.org/10.1016/j.tim.2011.01.001.
[24] S.K. Mishra, S. Choudhury, Experimental protocol for cecal ligation and puncture model of polymicrobial sepsis and assessment of vascular functions in mice, Methods Mol. Biol. 1717 (2018) 161–187, https://doi.org/10.1007/978-1-4939-7526-6_14.
[25] M.K. ElZarrad, P. Mukhopadhyay, N. Mohan, E. Hao, M. Dokmanovic, D.S. Hirsch, Y. Shen, P. Pacher, W.J. Wu, Trastuzumab alters the expression of genes essential for cardiac function and induces ultrastructural changes of cardiomyocytes in mice, PLoS One 8 (11) (2013) e79543, , https://doi.org/10.1371/journal.pone.0079543.
[26] Z.Q. Zhang, X.X. Wang, J.B. Gong, R. Zhan, X.J. Gao, Y. Zhao, L. Wu, X. Leng, L.J. Qian, Effects of HIP in protection of HSP70 for stress-induced cardiomyocytes injury and its glucorticoid receptor pathway, Cell Stress Chaperones 19 (6) (2014) 865–875, https://doi.org/10.1007/s12192-014-0510-y (2014).
[27] G. Chimienti, A. Picca, G. Sirago, F. Fracasso, R. Calvani, R. Bernabei, F. Russo, C.S. Carter, C. Leeuwenburgh, V. Pesce, E. Marzetti, A.M.S. Lezza, Increased TFAM binding to mtDNA damage hot spots is associated with mtDNA loss in aged rat heart, Free Radic. Biol. Med. 124 (2018) 447–453, https://doi.org/10.1016/j.freeradbiomed.2018.06.041.
[28] F. Fattahi, P.A. Ward, Complement and sepsis-induced heart dysfunction, Mol. Immunol. 84 (2017) 57–64, https://doi.org/10.1016/j.molimm.2016.11.012.
[29] F. Li, F. Lang, H. Zhang, L. Xu, Y. Wang, E. Hao, Role of TFEB mediated autophagy, oxidative stress, inflammation, and cell death in endotoxin induced myocardial toxicity of young and aged mice, Oxidative Med. Cell. Longev. 2016 (2016) 5380319, , https://doi.org/10.1155/2016/5380319.
[30] G. Stanzani, M.R. Duchen, M. Singer, The role of mitochondria in sepsis-induced cardiomyopathy, Biochim. Biophys. Acta Mol. basis Dis. 1865 (4) (2019) 759–773, https://doi.org/10.1016/j.bbadis.2018.10.011.
[31] D. Tsikas, Assessment of lipid peroxidation by measuring malondialdehyde (MDA) and relatives in biological samples: analytical and biological challenges, Anal. Biochem. 524 (2017) 13–30, https://doi.org/10.1016/j.ab.2016.10.021.
[32] X. Yao, D. Carlson, Y. Sun, L. Ma, S.E. Wolf, J.P. Minei, Q.S. Zang, Mitochondrial ROS induces cardiac inflammation via a pathway through mtDNA damage in a pneumonia-related sepsis model, PLoS One 10 (10) (2015) e0139416, , https://doi.org/10.1371/journal.pone.0139416.
[33] D. Heras-Sandoval, J.M. Perez-Rojas, J. Hernandez-Damian, J. Pedraza-Chaverri, The role of PI3K/AKT/mTOR pathway in the modulation of autophagy and the clearance of protein aggregates in neurodegeneration, Cell. Signal. 26 (12) (2014) 2694–2701, https://doi.org/10.1016/j.cellsig.
[34] M.P. Myers, I. Pass, I.H. Batty, J. Van der Kaay, J.P. Stolarov, B.A. Hemmings, M.H. Wigler, C.P. Downes, N.K. Tonks, The lipid phosphatase activity of PTEN is critical for its tumor supressor function, Proc. Natl. Acad. Sci. U. S. A. 95 (23) (1998) 13513–13518.
[35] F. Li, F. Lang, H. Zhang, L. Xu, Y. Wang, C. Zhai, E. Hao, Apigenin alleviates endotoxin-induced myocardial toxicity by modulating inflammation, oxidative stress, and autophagy, Oxidative Med. Cell. Longev. 2017 (2017) 2302896, , https://doi.

org/10.1155/2017/2302896.
[36] H.M. Li, K.Y. Li, Y. Xing, X.X. Tang, D.M. Yang, X.M. Dai, D.X. Lu, H.D. Wang, Phenylephrine attenuated sepsis-induced cardiac inflammation and mitochondrial injury through an effect on the PI3K/Akt signaling pathway, J. Cardiovasc. Pharmacol. 73 (3) (2019) 186–194, https://doi.org/10.1097/FJC.0000000000000651.
[37] X. Shang, J. Li, R. Yu, P. Zhu, Y. Zhang, J. Xu, K. Chen, M. Li, Sepsis-related myocardial injury is associated with Mst1 upregulation, mitochondrial dysfunction and the Drp1/F-actin signaling pathway, J. Mol. Histol. 50 (2) (2019) 91–103, https://doi.org/10.1007/s10735-018-09809-5.
[38] M.T. Chung, Y.M. Lee, H.H. Shen, P.Y. Cheng, Y.C. Huang, Y.J. Lin, Y.Y. Huang, K.K. Lam, Activation of autophagy is involved in the protective effect of 17beta-oestradiol on endotoxaemia-induced multiple organ dysfunction in ovariectomized rats, J. Cell. Mol. Med. 21 (12) (2017) 3705–3717, https://doi.org/10.1111/jcmm.13280.
[39] P. Li, X.R. Chen, F. Xu, C. Liu, C. Li, H. Liu, H. Wang, W. Sun, Y.H. Sheng, X.Q. Kong, Alamandine attenuates sepsis-associated cardiac dysfunction via inhibiting MAPKs signaling pathways, Life Sci. 206 (2018) 106–116, https://doi.org/10.1016/j.lfs.2018.04.010.
[40] W.X. Zhang, B.M. He, Y. Wu, J.F. Qiao, Z.Y. Peng, Melatonin protects against sepsis-induced cardiac dysfunction by regulating apoptosis and autophagy via activation of SIRT1 in mice, Life Sci. 217 (2019) 8–15, https://doi.org/10.1016/j.lfs.2018.11.055.
[41] R. An, L. Zhao, C. Xi, H. Li, G. Shen, H. Liu, S. Zhang, L. Sun, Melatonin attenuates sepsis-induced cardiac dysfunction via a PI3K/Akt-dependent mechanism, Basic Res. Cardiol. 111 (1) (2016) 8, , https://doi.org/10.1007/s00395-015-0526-1.
[42] C. Li, F. Hua, T. Ha, K. Singh, C. Lu, J. Kalbfleisch, K.F. Breuel, T. Ford, R.L. Kao, M. Gao, T.R. Ozment, D.L. Williams, Activation of myocardial phosphoinositide-3-kinase p110alpha ameliorates cardiac dysfunction and improves survival in polymicrobial sepsis, PLoS One 7 (9) (2012) e44712, , https://doi.org/10.1371/journal.pone.0044712.
[43] E. Zhang, X. Zhao, L. Zhang, N. Li, J. Yan, K. Tu, R. Yan, J. Hu, M. Zhang, D. Sun, L. Hou, Minocycline promotes cardiomyocyte mitochondrial autophagy and cardiomyocyte autophagy to prevent sepsis-induced cardiac dysfunction by Akt/mTOR signaling, Apoptosis (2019), https://doi.org/10.1007/s10495-019-01521-3.
[44] J. Zhang, P. Zhao, N. Quan, L. Wang, X. Chen, C. Cates, T. Rousselle, J. Li, The endotoxemia cardiac dysfunction is attenuated by AMPK/mTOR signaling pathway regulating autophagy, Biochem. Biophys. Res. Commun. 492 (3) (2017) 520–527, https://doi.org/10.1016/j.bbrc.2017.08.034.
[45] W. Han, H. Wang, L. Su, Y. Long, N. Cui, D. Liu, Inhibition of the mTOR pathway exerts cardioprotective effects partly through autophagy in CLP rats, Mediat. Inflamm. 2018 (2018) 4798209, , https://doi.org/10.1155/2018/4798209.
[46] Y. Zhang, X. Xu, A.F. Ceylan-Isik, M. Dong, Z. Pei, Y. Li, J. Ren, Ablation of Akt2 protects against lipopolysaccharide-induced cardiac dysfunction: role of Akt ubiquitination E3 ligase TRAF6, J. Mol. Cell. Cardiol. 74 (2014) 76–87, https://doi.org/10.1016/j.yjmcc.2014.04.020.
[47] G.L. Gravina, L. Biordi, F. Martella, V. Flati, E. Ricevuto, C. Ficorella, V. Tombolini, C. Festuccia, Epigenetic modulation of PTEN expression during antiandrogenic therapies in human prostate cancer, Int. J. Oncol. 35 (5) (2009) 1133–1139.
[48] U. Jambalganiin, B. Tsolmongyn, N. Koide, E. Odkhuu, Y. Naiki, T. Komatsu, T. Yoshida, T. Yokochi, A novel mechanism for inhibition of lipopolysaccharide-induced proinflammatory cytokine production by valproic acid, Int. Immunopharmacol. 20 (1) (2014) 181–187, https://doi.org/10.1016/j.intimp.2014.02.032.
[49] C.T. Lin, H.C. Lai, H.Y. Lee, W.H. Lin, C.C. Chang, T.Y. Chu, Y.W. Lin, K.D. Lee, M.H. Yu, Valproic acid resensitizes cisplatin-resistant ovarian cancer cells, Cancer Sci. 99 (6) (2008) 1218–1226, https://doi.org/10.1111/j.1349-7006.2008.00793.x.
[50] J.H. Lee, A. Mahendran, Y. Yao, L. Ngo, G. Venta-Perez, M.L. Choy, N. Kim, W.S. Ham, R. Breslow, P.A. Marks, Development of a histone deacetylase 6 inhibitor and its biological effects, Proc. Natl. Acad. Sci. U. S. A. 110 (39) (2013) 15704–15709, https://doi.org/10.1073/pnas.1313893110.
[51] I. Oehme, J.P. Linke, B.C. Bock, T. Milde, M. Lodrini, B. Hartenstein, I. Wiegand, C. Eckert, W. Roth, M. Kool, S. Kaden, H.J. Grone, J.H. Schulte, S. Lindner, A. Hamacher-Brady, N.R. Brady, H.E. Deubzer, O. Witt, Histone deacetylase 10 promotes autophagy-mediated cell survival, Proc. Natl. Acad. Sci. U. S. A. 110 (28) (2013) E2592–E2601, https://doi.org/10.1073/pnas.1300113110.
[52] Y. Wang, P. Chen, L. Wang, J. Zhao, Z. Zhong, Y. Wang, J. Xu, Inhibition of histone deacetylases prevents cardiac remodeling after myocardial infarction by restoring autophagosome processing in cardiac fibroblasts, Cell. Physiol. Biochem. 49 (5) (2018) 1999–2011, https://doi.org/10.1159/000493672.
[53] F. Yang, F. Wang, Y. Liu, S. Wang, X. Li, Y. Huang, Y. Xia, C. Cao, Sulforaphane induces autophagy by inhibition of HDAC6-mediated PTEN activation in triple negative breast cancer cells, Life Sci. 213 (2018) 149–157, https://doi.org/10.1016/j.lfs.2018.10.034.